EXPLOSIVE FORMING STRESS ANALYSIS

PHASE II

RYAN

AERONAUTICAL COMPANY

EXPLOSIVE FORMING STRESS ANALYSIS

PHASE II

RYAN

AERONAUTICAL COMPANY

REPORT NO. 64B021
21 FEBRUARY 1964

PAGES 36

COPY NO. 27

REVISIONS: Insert latest changed pages. Destroy superseded pages.

Page No.	Date

Prepared By: R. W. Johnson
R. W. Johnson
Senior Structures Engineer

Approved By: H. F. Wallen
H. F. Wallen
Chief Tool Engineer

Approved By:
K. D. Hawkins
Chief Manufacturing
Technical Development

RYAN 64B021

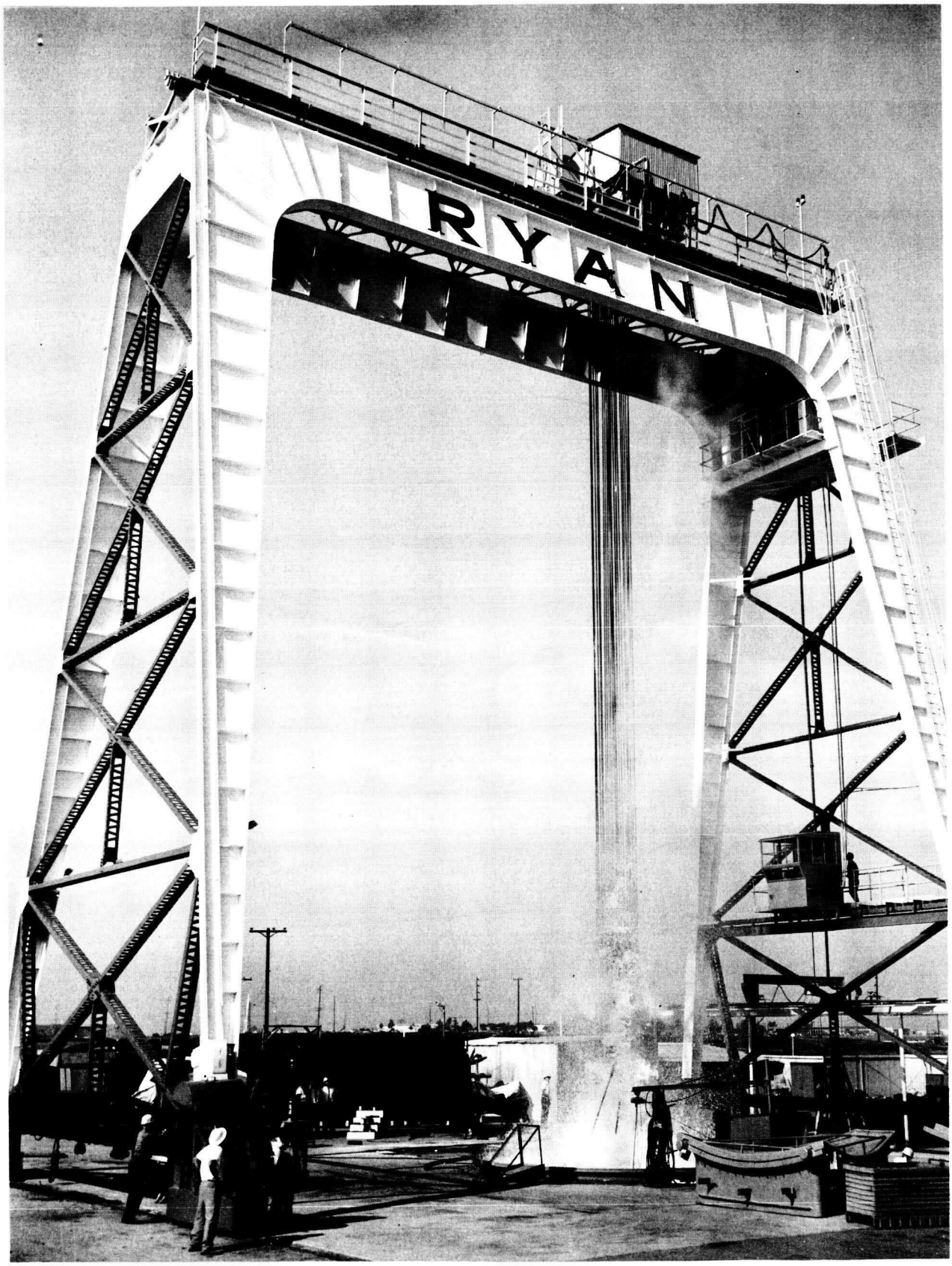
RYAN

ABSTRACT

29224

This report is Phase II which presents additional data and methods of analysis for use in explosive forming. The task was performed by Ryan Aeronautical Company in conjunction with NASA Contract Number NAS 8-5129.

An explosive forming tank is analyzed by the impulse method developed in Phase I (Ref. 1), and was found adequate for Phase III use. Notable is the fact that no "factor of ten", or some such number as reported by others, (Ref. 8, Page 264) is resorted to in the new tank analysis method.

Sub-scaled sized plates, except for thickness, were explosively formed. The charge size calculated in Ref. 1 was used successfully to form the .80 inch-thick, 2219-T37 aluminum plate in the sub-scale die. Full-scale stretch press wedge clamps were successful in retaining the part in the sub-scale die.

Discussions of explosives, impact phenomena, and stress wave propagation are included.

Author

CONTENTS

SYMBOLS

a	Time constant
c	Speed of sound, ft./sec.
E	Modulus of elasticity, psi.
f	Coefficient of friction
F	Force, lb.
g	Gravitational acceleration, 386 in./sec./sec.
g	Grams (1 g = 15.43 gr)
gr	Grains (1 lb. = 7000 gr)
I	Impulse, lb.-sec.
m	Mass, slugs
m	Milli (ms = milliseconds)
M	Mass, slugs
p	Pressure, psi.
p	Natural circular frequency, rad./sec. (See also ω.)
P	Load, lb.
R	Radius, inches
s	Distance between two charges, ft.
S	Distance from cg of charge to surface of part in feet
t	Time, microseconds
U	Energy, in. lb.
v	Velocity, ft./sec.
v	Volume, cu. ft.
w	Distributed load, lb./in. (See also ω.)
w	Density, lb./cu. in.
W	Weight of explosive charge, lb.

x	Deflection, inches
$\dot{x}$	dx/dt
$\ddot{x}$	$d\dot{x}/dt$
a	Acceleration, in./sec./sec.
ρ	Mass density, slugs/cu. ft.
μ	Micro (μS = microseconds)
ν	Poisson's ratio
σ	Normal stress, psi.
τ	Shear stress, psi.
ϵ	Strain, in./in.
$\dot{\epsilon}$	Strain rate, in./in./sec.
δ	Deflection, inches
ω	Forcing frequency, rad/sec.

USEFUL CONVERSION FACTORS

1 in./sec. = 2.54 cm/sec.

1 g/cc = .0362 lb./cu. in.

1 meter = 3.28 ft. = 39.4 in.

1 micron = .001 millimeter

1 cal./g = 1.7988 Btu/lb.

1 Btu = 778.156 ft.-lb.

1 Btu = 1054.866 int. joules

1 kg/sq. cm. = 14.2234 psi

1 Angstrom = 10^{-4} microns

LIST OF FIGURES

INTRODUCTION

This Phase II report concerns a 3-phase Research and Development Program. Sub-scale explosive forming tests were conducted according to Phase II of Ref. 7, Page 14. Full-scale, "jury-rigged" shots were also made on the base gores during this same period. Observations from both of these operations aided in planning the Phase III Research and Development Program. Phase III is the full-scale production phase of both the base and apex gores for the NASA Saturn V Gore Explosive Forming Program.

Symbols and formulae used are in many cases taken from Ref. 1, the Phase I report.

The sub-scale explosive forming tests verified the use of stretch-press wedge clamps, and the size of the charge.

1.0 WELDING

Experience at Ryan shows that welds of aluminum and of steel are not detrimental in stand-off operations if proper welding procedures are used. A conclusion of this in the light of the unfortunate experiences of others, is that good welding technology prevents failures. The weld strength is apparently a function of the men and equipment doing the welding, as well as careful design of the welded joints. If one of the three is faulty - the man, the equipment, or the structural design - a failure may occur.

2.0 STRESS ANALYSIS OF EXPLOSIVE FORMING TANK

Conventional methods of analysis do not give reliable results. If the conventional method of analysis based on static stresses was valid, Ryan's tank would have ruptured during prior tests. Instead, the strain energy method of analysis must be used as in Ref. 1. A second method, also discussed in Ref. 1, is the impulse-kinetic energy method of approach. Both of these methods hold in the elastic region (i.e., below the yield stress) and must be modified in the tank yields. Since an explosive-forming tank is not supposed to yield, the post-yield methods of analysis need not be developed.

The tank analysis that follows is based on the Primacord charges being located at the same elevation in the tank, each cord of the same explosive loading, equal spacing between cords, and all cords fired at the same instant:

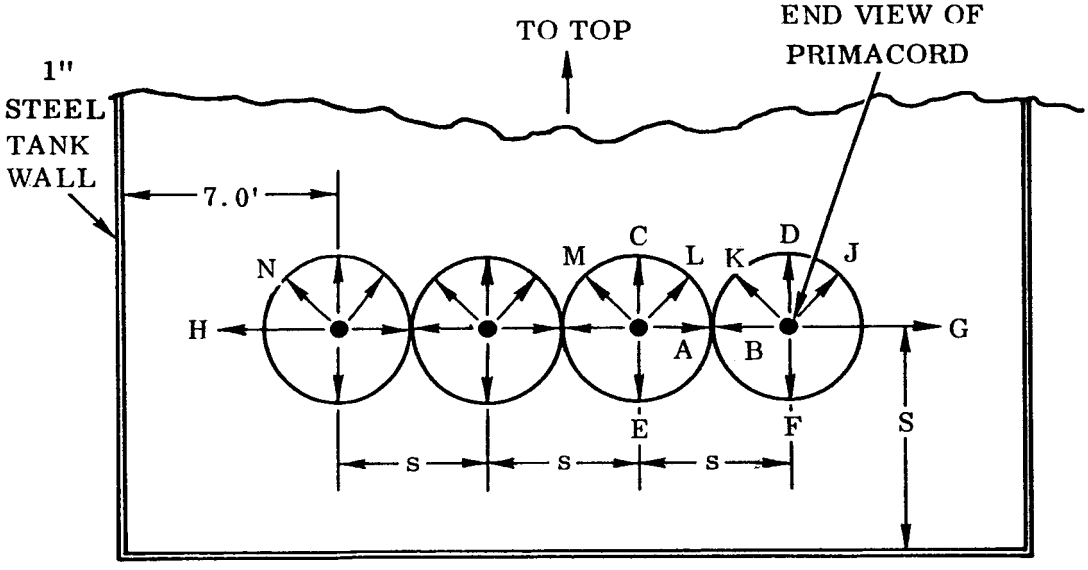

Figure 1 Sketch of Tank - Die Not Shown

Pressure waves A and B cancel. Walls of tank will feel only G, H, J and N. Vertical pressures, (C and D types) go out the top as a plume. K and L types add and go out the top with C and D. It is assumed that

the pressure waves going downwards are used to form the metal blank in the die (not shown).

2.1 ENERGY ANALYSIS OF TANK

This method is outlined on pages 5 through 9 of Ref. 1. Refer to Equations 2.1 and 3.3 of Ref. 1. The energy available from the charge of 2000 grains per foot is:

$$U = 3270\ W/S^2 = 3270\ (.214)/(7)^2 = 14.3 \text{ in. lb./sq. in.}$$

(Where stand-off from the tank wall is 7 feet)

The stress produced by this energy at the tank wall is:

$$\sigma_x = \sqrt{2\ EU} = \sqrt{2 \times 29 \times 10^6 \times 14.3} = 28,800 \text{ psi}$$

M. S. = Adequate

Note that this stress is within the elastic limit and the formula holds. Also, the tank is 1.0 inch thick, so it has a volume of one cubic inch for each square inch of surface area. The sand around the tank is conservatively neglected.

2.2 IMPULSE ANALYSIS OF TANK

This method is outlined on Page 23-24 of Ref. 1. Refer to Equations 3.1 and 5.6 of Ref. 1. The impulse available from the 2000 grain per foot charge at the tank wall 7 feet away is:

$$I = 2.18\ (.214)^{2/3}/(7) = .1115 \text{ lbs.-sec./sq. in.}$$

The stress in the tank wall due to the impulse is:

$$\sigma_x = I\sqrt{\frac{Eg}{Wv}} = (.1115)\sqrt{\frac{29 \times 10^6 \times 386}{1.0 \times .283 \times 1.0}} = 22,200 \text{ psi}$$

M. S. = Adequate

Note that if the weight and volume of the sand around the tank were included, the stress would be considerably reduced.

2.3 PRESSURE ANALYSIS OF TANK

Equation 3.2 of Ref. 1 shows the pressure exerted on the tank wall for a 2000 grain per foot Primacord charge:

$$p = 22,000\ (.214)^{1/3}/(7) = 1880 \text{ psi}$$

The hoop tension in the wall is obtained from the classical thin-walled cylinder formula (Page 295, Ref. 16):

$$\sigma_x = pR/t = (1880)\ (150)/1.0 = 282,000 \text{ psi}$$

With this method of analysis a positive margin of safety is obtained only by using some factor, e.g., ten (10), on the allowable stress. Obviously, the energy method is preferable. The pressure method is applicable for static loads and is misleading for explosive forming.

Ryan's experience with large explosive charges, symmetrically located, bears this out. The explosive forming tank would have ruptured if such a pressure method was valid.

3.0 EXPLOSIVES AVAILABLE

Additional data is presented for those unfamiliar with explosive forming. No endorsements of any particular products are intended, either here or in the Phase I report. This section supplements data given in the Phase I report (Ref. 1) on Pages 26 through 28.

3.1 DUPONT DETASHEET CORD

This extruded cord explosive is available up to 3 inches in diameter, which is equivalent to about 2000 grains per foot. It may be used in place of Primacord, for example, because the maximum standard Primacord loading is only 400 grains per foot. Hence, one 3-inch diameter Detasheet cord may be equivalent to five PETN 400 grains per foot Primacords.

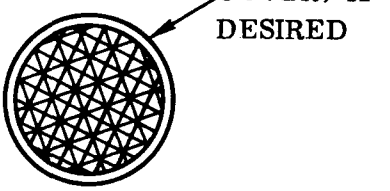

Figure 2 Detasheet Cord

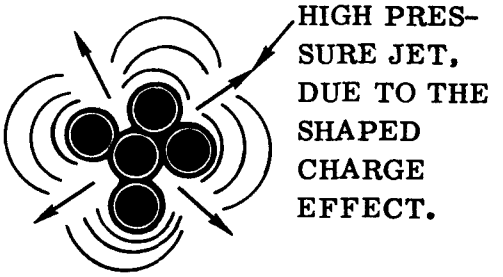

Figure 3 Primacord

3.2 DUPONT DETASHEET D (PLASTIC SHEET)

The smallest size available (on special order) is .015 inch thick and has an explosive loading of about 1/3 grams per square inch.

3.3 DUPONT DETASHEET C (PLASTIC SHEET)

Another size that may be useful for explosive forming is only .025 inch thick and weighs 5/8 grams per square inch. By completely covering an area with this Detasheet, a large quantity of uniformly distributed explosive is made available. A feel for the over-all loading of this plastic sheet can be obtained by multiplying a typical gore area times the sheet weight:

15,000 x .625 x 15.43/7000 = 20.7 lb. explosive weight

This quantity of explosive is considered quite high for explosive forming. Consequently, Detasheet D (above) may be preferable as a more useful size.

3.4 BLASTING CAPS

Only electrically actuated caps are listed. The charges in the caps are small and can often be neglected.

CAP	CHARGE
DuPont E-94	2 gr.
#6	4.9 gr.
#8	6.9 gr.
Engineer's Special	13.9 gr. (minimum)

Ryan uses the Engineer's Special, since the cost differential is small and this size assures detonation. In addition, resistors are provided, which require 45 volts to fire these caps, and offers an extra safety precaution at Ryan.

4.0 IMPACT PHENOMENA

There are many definitions of impact. For this reason, several definitions and examples are discussed on the following pages. Note that in some cases an explosive formed part is not strictly under impact of any one kind. The part may be under a "static" loading according to one definition, but the loading may be classed as "impact" if one of the other definitions is used.

It is suggested that a part be classed as being under impact if it satisfies one of the following definitions, even though it does not satisfy any of the other definitions.

4.1 TIME OF IMPULSE VERSUS NATURAL PERIOD

If the natural period $2\pi/p$ is much longer than the time it takes for the blast pressure wave to hit the part, then the deflection is proportional to the impulse, I. If the natural period is "fast" compared with pressure wave time, then the deflection is proportional to pressure, i.e., quasi-static. This is stated by Cole, (6), Page 417. Jacobsen & Ayre (9) also use this criteria for mechanical systems. Ref. 1 (Pages 14 and 23) used this criteria as a basis for its impulsive analysis.

4.2 TIME OF IMPULSE VERSUS SHOCK WAVE TRAVEL TIME

Consider a tensile specimen. The stress at one end is zero and at the other equals σ. A stress wave will travel to the unloaded end at the velocity of sound in the material. The wave will be reflected and may travel back and forth along the specimen several times. Eventually, it dies out leaving uniform tension end to end.

In impact loading, the specimen may break at one end before the stress is felt at the other.

The speed of sound in 2219-T37 is 254,000 inches per second, Table I. It takes .8/254,000 = 3.14 microseconds for the stress to travel through an .80 inch thick plate. Now, since it takes 20 microseconds to 50 microseconds for a blast to reach its peak pressure, this case may be considered as a "non-impact" type of loading, (Pages 16-17, Ref. 5a), because the load is applied slowly compared with the time it takes the stress wave to travel through the part.

The classification as "non-impact" could be applied to the water blast pressure wave effect as it passes through the plate as discussed in the above paragraph (Figure 4); but, for actual stretching of the plate laterally, this does not apply (Figure 5). See Section 4.3.

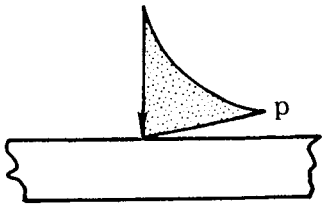

Figure 4 Compression Normal To Plane of the Plate

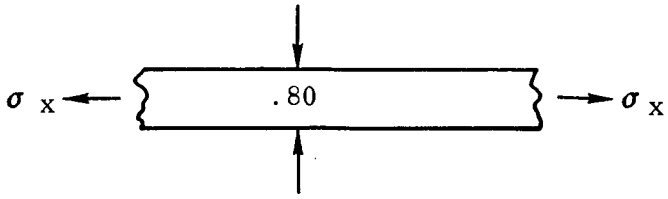

Figure 5 Tension in Plane of the Plate During Forming

The speed of sound in the die is about 228,000 inches per second, and it is generally 7.0 inches thick. Time to travel through 7.0 inches is t = 7.0/228,000 = 30.6 microseconds. The time for the reflected wave to return back through 7.0 inches is an additional 30.6 microseconds if attenuation and dispersion is neglected. The blast shock wave has a rise time of 20 to 50 microseconds. The rise time as used here is less than the stress wave propagation time of 61.2 microseconds. In this case, the die is more in the impact region than the aluminum plate (Figure 4), from the viewpoint of stress wave propagation only.

Impact is characterized by an elastic phase and then a plastic phase. Many materials tested conventionally by Izod or Charpy tests absorb 70% of the total impulse (Pages 88-89 of Ref. 5b) after yielding. Conventional tests are hence not a good single measure of impact resistance if yielding alone is a criteria.

Under impact, an increase in area may weaken a member instead of strengthening it (Page 82, Ref. 4).

4.3 TIME OF IMPULSE VERSUS STRAIN RATE

Another way of considering impact is from the viewpoint of strain rates. The average strain rate on the part is determined by the time to bottom out on the die, and the probable maximum strain in the metal (Figure 5) at that time. The strain rate on the die is found by dividing the maximum strain of the die, by the time it takes to reach that maximum

strain, which results in the average strain rate. The latter was done in Ref. 1. The former is done in the following computation.

The shock wave strains (Figure 4) must be differentiated from the actual "stretching" strains (Figure 5) in dealing with strain rates.

Calculation of Metal-Forming Time

The time for the metal to be formed is defined as the time from the instant the water shock wave first hits the aluminum part until the part hits the bottom of the die cavity and stops.

The method of computing this time follows:

$$v = \alpha t \qquad \text{(Equation 1)}$$

$$F = m\alpha = \frac{W\alpha}{g} \quad \text{or,} \quad \alpha = \frac{Fg}{W} \qquad \text{(Equation 2)}$$

thus $$v = \frac{Fgt}{W} = \frac{Ig}{W} \qquad \text{(Equation 3)}$$

now, the distance the part travels is denoted by d:

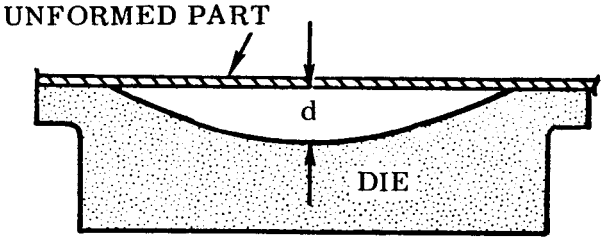

Figure 6 Sketch Showing Distance Part Must Travel

and, $d = vt$ (Equation 4)

or, $t = d/v = dW/Fgt$ (Equation 5)

and, noting that Impulse, $I = Ft$ (Equation 6)

obtain finally $t = Wd/Ig = Wd/I\ (386)$ (Equation 7)

where W is weight of part per square inch,

d is in inches, and I is lb. sec./sq. in.

Forming Time for .80 Aluminum Plate

From Equation 7:

$$t = Wd/Ig = \frac{(.102)\ (.8)\ (13)}{(1.04)\ (386)} = .0264 \text{ sec.}$$

where d is assumed a 13-inch deep cavity in the die.

$$I = 2.18\ (.214)^{2/3}/.75 = 1.04 \text{ lb.-sec./sq.in.}$$

and from Equation 3:

$$v = \frac{Ig}{W} = \frac{(1.04)\ (386)}{(.102)\ (.8)} = 4910 \text{ in./sec.}$$

Hence, it takes .026 seconds for the plate to form, assuming no edge restraint which would slow the process down. Also, the vacuum under the part must remain a vacuum during this time.

Strain Rate

Assuming the plate is elongated 3% during this time, the strain rate is .03/.026 = 1.15 in./in./sec. which is 115%/sec. This is about a hundred times faster than a typical "static" rate, Figure 15, Ref. 1.

Plate Velocity = 4910/12 = 410 ft./sec.

This velocity is similar to those on Page 271 of Ref. 8 (they are all approximately 400 ft./sec.).

Note that a "high" impulse is like a "fast" impulse; the forming takes place more quickly.

5.0 PROPAGATION OF STRESS WAVES

The existing literature on explosive forming separates water shock waves from shock waves in solids. This report uses a "structural" approach, i.e., the stress waves in air, water, wood, concrete, aluminum and steel are treated similarly. This is predicated on all these materials being incompressible at the stresses (or pressure, which is also psi) encountered in the stand-off operations herein concerned. Hence, all material densities are considered constant, and can be used in the "solid theory" stress wave formulae.

5.1 HYDRODYNAMIC VERSUS SOLID THEORY

Wave propagation in a solid based on hydrodynamic theory (at high pressures) has no shear wave. Hence, when striking boundaries, there is no reflected shear wave as there would be in the "solid" theory mentioned in the previous paragraph. This is mentioned, because in contact operations, as opposed to stand-off operations, high pressures up to 5,000,000 psi are generated at the explosive-metal interface. For such high pressures, the density and rigidity of a material are increased. These increases change the speed of wave propagation among other things.

Compressibility

From Nadai, the hydrostatic compressibility of aluminum is given as:

$$\frac{\Delta v}{v_o} = 10^{-7}p\,(13.34 - 3.5 \times 10^{-5}p)$$ (Page 33, Ref. 13) (Equation 8)

For 1000 atmospheres (which is 1000 kg/sq. cm.) the pressure p = 14,200 psi as given by Nadai. Such a pressure (14,200 psi) is typical for stand-off operations as opposed to contact operations which may have a pressure in the order of 3×10^6 psi.

To illustrate the compressibility substitute p = 1000 kg/sq. cm. into Equation 8 to obtain:

$$\frac{\Delta v}{v_o} = 10^{-4}\,(13.34 - 3.5 \times 10^{-2}) = .001331 \text{ cu. in./cu. in.}$$

Hence, for all practical purposes as compared to the strain in metal the compressibility can be neglected and the density is constant.

The Hugoniot curves (Page 131, Ref. 8) relating volume change to pressure are hence not usually needed for stand-off operations. The Rankine-Hugoniot relations for pressure versus density also are not needed (Page 30, Ref. 20).

While on the subject of simplifying the theory, the Chapman-Jouget condition is also mentioned. Cole (Page 71, Ref. 6) states that the Chapman-Jouget condition is for the detonation process and holds only for a self-sustaining process, such as detonation along the length of a Primacord. Hence, since the investigation at hand is stress wave propagation and not detonation itself, the Chapman-Jouget relation is not needed.

5.2 LONGITUDINAL WAVES

Longitudinal waves only will be considered in this report. Note that a longitudinal wave can be transformed completely into a shear wave.

The method of superposition is valid, because waves are linear; however, this is valid only for elastic waves. Plastic wave fronts propagate at slower speeds than elastic strain waves. For stand-off operations, the explosive wave pressure at the surface of the blank produces less than the yield compressive stress in the aluminum which it propagates into. Hence, the stress waves are elastic and von Karman's equation (Page 5, Ref. 21) holds:

$$\sigma = \rho \, cv \qquad \text{(Equation 9)}$$

For plastic waves, which are not dealt with here, see also Ref. 21.

Because water can resist very little tensile stress, this equation holds for water only in a state of compression.

A transmitted wave always has the same sign as the incident stress. The reflected wave will change sign if the "bearing" material is "softer". If the bearing block is "harder", then the reflected wave stress has the same sign.

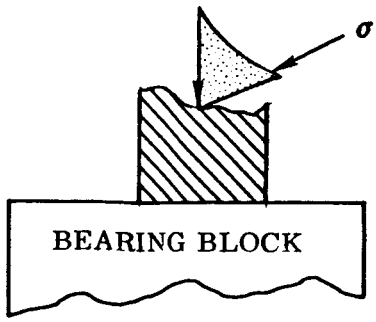

Figure 7 Incident Stress Wave Moving Towards a Supporting Member

The lengths of the stress waves in two different mediums will not be the same due to dissimilar wave propagation speeds.

5.2.1 Longitudinal Waves at a Discontinuity

The following is based on elementary theory derived by Rayleigh for an infinite bar with steady state wave propagation (Chapter 7, Volume I, Ref. 14).

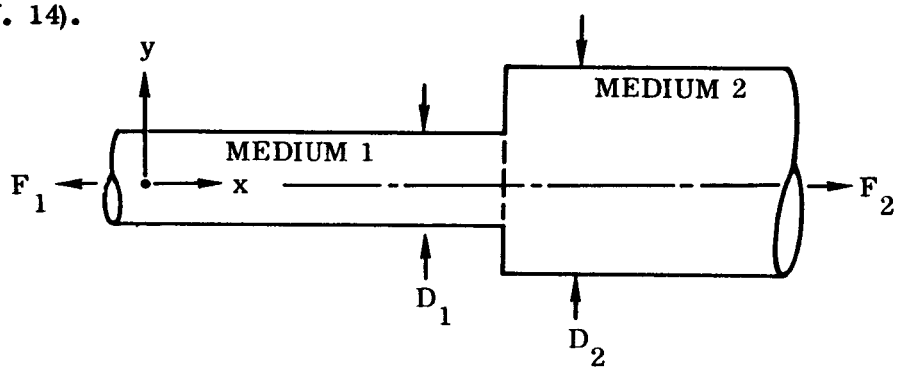

Figure 8 Stress Wave Propagation From One Material Into Another

The stress is in Medium 1 and moving into Medium 2, which has a different area for the most general case.

$$\frac{E}{\rho} \frac{\partial^2 u}{\partial x^2} = \frac{\partial^2 u}{\partial t^2}$$

Where u is displacement in x-direction (Equation 10)

$$\frac{EI}{\rho A} \frac{\partial^4 y}{\partial x^4} = \frac{\partial^2 y}{\partial t^2} \quad \text{(Equation 11)}$$

$$F_1 = F_2 \quad \text{(Equation 12)}$$

$$v_1 = v_2 \quad \text{(Particle Velocity)} \qquad \text{(Equation 13)}$$

Now, let σ_1 = Stress in incident pulse

σ_1' = Stress in reflected pulse

σ_2' = Stress in transmitted pulse

From Equations 10 and 12 obtain $(\sigma_1 + \sigma_1')\ A_1 = \sigma_2' A_2$ (Equation 14)

and

$$v_1 - v_1' = v_2' \qquad \text{(Equation 15)}$$

Now, from elementary theory, the bar velocity $c = \sqrt{E/\rho}$
and from Equation 9, $\sigma = \rho c v$

Solving Equations 14, 15 and 9 obtain

$$\sigma_1' = \frac{\rho_2 A_2 c_2 - \rho_1 A_1 c_1}{\rho_1 A_1 c_1 + \rho_2 A_2 c_2} \cdot \sigma_1 \qquad \text{(Equation 16)}$$

$$\sigma_2' = \frac{2\ \rho_2 A_1 c_2}{\rho_1 A_1 c_1 + \rho_2 A_2 c_2} \cdot \sigma_1 \qquad \text{(Equation 17)}$$

Equations 16 and 17 are from Ref. 15 and are for the most general case. For the case where mediums 1 and 2 are the same but with different areas, the equations reduce to:

$$\sigma_1' = \frac{A_2 - A_1}{A_1 + A_2} \cdot \sigma_1 \qquad \text{(Equation 18)}$$

$$\sigma_2' = \frac{2 A_1}{A_1 + A_2} \cdot \sigma_1 \qquad \text{(Equation 19)}$$

Equations 18 and 19 show that if there is an increase in cross-section that the reflected wave has the same sign. The reflected wave has the opposite sign if the area is decreased.

For the case where the areas are the same and the materials differ, Equations 16 and 17 reduce to:

$$\sigma_1' = \frac{\rho_2 c_2 - \rho_1 c_1}{\rho_1 c_1 + \rho_2 c_2} \cdot \sigma_1 \qquad \text{(Equation 20)}$$

$$\sigma_2' = \frac{2 \rho_2 c_2}{\rho_1 c_1 + \rho_2 c_2} \cdot \sigma_1 \qquad \text{(Equation 21)}$$

Equations 20 and 21 check with Ref. 8, Page 114, and will be used to illustrate the stress wave transmission through several mediums - air, water, wood, concrete, aluminum, and steel.

The mass density is contained in both numerators and denominators. Hence, the acceleration due to gravity, g, may be cancelled out. This is resorted to in Table I which lists the specific acoustic resistance as g ρ c, where ρ is mass density. These values can then be substituted into Equations 20 and 21 to determine the stress transmitted and reflected between 2 mediums of the same area.

TABLE I

MATERIAL	DENSITY, gρ LB./CU. IN.	SONIC SPEED, c IN./SEC.	g c ρ PSI/SEC.
Air	.00044	13,200	5.8
Fresh Water	.036	57,000	2060
Typical Wood	.018	152,500	2740
Concrete	.094	122,000	11400
2219 Aluminum	.102	254,000	25900
Die Steel	.283	228,000	64500
Earth		48,000	
Granite		156,000	

5.2.2 Speed of Stress Wave Propagation

Two materials are selected to illustrate the method of calculating the "plane" velocity of stress propagation. The equations are selected from Rinehart and Pearson (Ref. 8), which is highly recommended. Typical speeds are given in Table I.

Bulk Modulus, $K = E/3\,(1-2\nu)$ (Equation 22)

Dilatation Velocity, $c_L = \sqrt{\frac{3K}{\rho}\left(\frac{1-\nu}{1+\nu}\right)}$ (Equation 23)

Aluminum, 2219-T37

$$K = \frac{10.8 \times 10^6}{3\left[1-2\,(.34)\right]} = 11.28 \times 10^6 \text{ psi}$$

$$c_L = \sqrt{\frac{3 \times 11.28 \times 10^6\,(1-.34)}{\left(\frac{.102}{386}\right)\,(1+.34)}} = 254{,}000 \text{ in./sec.}$$

Where $\rho = w/g = .102/386$ (Table 3.2.25.0(b), Ref. 17)

$\nu = .34$ (Ref. 18)

$E = 10.8 \times 10^6$ (Table 3.2.25.0(b), Ref. 17)

Die Steel

Material properties are from Ref. 3

$$K = \frac{29 \times 10^6}{3\,(1-.6)} = 24.2 \times 10^6 \text{ psi}$$

$$c_L \sqrt{\frac{3\,(24.2 \times 10^6)\,386\,(.7)}{(.283)\,(1.3)}} = 228{,}000 \text{ in./sec.}$$

5.2.3 Partition of Stress

The longitudinal stress wave propagating at the speed of sound in a medium will be partially reflected from the juncture with a second medium. If the second medium is a vacuum, then the entire stress wave is reflected, with the sign of the stress being changed. An infinitely stiff second medium reflects the entire wave unchanged in sign (Ref. 19), in which case the incident wave and reflected wave will add because they are of the same sign.

Calculation of Reflected and Transmitted Stress Waves

The incident longitudinal propagating stress wave, σ_1, divides into two propagating waves upon striking a boundary. These two waves are, σ'_1, the reflected stress wave in the original part, and σ'_2, the transmitted stress wave in the second material. Sample calculations are shown to illustrate the method using two different materials but assuming equal areas.

Aluminum to Steel

The values of Table I are substituted into Equations 20 and 21 to obtain:

$$\sigma'_1 = \frac{64,500 - 25,900}{90,400} \quad \sigma_1 = .43 \quad \sigma_1$$

$$\sigma'_2 = \frac{2\,(64,500)}{90,400} \quad \sigma_1 = 1.43 \quad \sigma_1$$

The original stress in the aluminum is reflected and reduced to 43%. The stress transmitted into the steel is increased to 143% of that in the aluminum.

Steel to Water

$$\sigma'_1 = \frac{2060 - 64,500}{66,560} \quad \sigma_1 = -.94 \quad \sigma_1$$

$$\sigma'_2 = \frac{2\,(2060)}{66,560} \quad \sigma_1 = .06 \quad \sigma_1$$

The incident stress in the steel, if compression, becomes tension when it is reflected from the die-water interface back into the steel. Only 6%

is transmitted into the water, showing that water is not much of a cushion under the die overhang.

Steel to Air

$$\sigma_1' = \frac{5.8 - 64,500}{64,506} \sigma_1 = -1.0 \sigma_1$$

$$\sigma_2' = \frac{2(5.8)}{64,506} \sigma_1 = .00018 \sigma_1$$

Air transmits little, if any. The entire stress wave is reflected back into the steel with a sign change. Hence, water is 6% better than air in this respect. By providing vents into die areas that may have entrapped air, the reflected stress in the die is reduced.

Steel to Wood

$$\sigma_1' = \frac{2740 - 64,500}{67,240} \sigma_1 = -.92 \sigma_1$$

$$\sigma_2' = \frac{2(2740)}{67,240} \sigma_1 = .08 \sigma_1$$

Steel to Aluminum

$$\sigma_1' = \frac{25,900 - 64,500}{90,400} \sigma_1 = .43 \sigma_1$$

$$\sigma_2' = \frac{51,800}{90,400} \sigma_1 = .57 \sigma_1$$

Steel to Concrete

$$\sigma_1' = \frac{11,400 - 64,500}{75,900} \sigma_1 = -.70 \sigma_1$$

$$\sigma_2' = \frac{22,800}{75,900} \sigma_1 = .30 \sigma_1$$

Water to Aluminum

$$\sigma_1' = \frac{25,900 - 2060}{27,960} = .85\ \sigma_1$$

$$\sigma_2' = \frac{2\ (25,900)}{27,960} = 1.85\ \sigma_1$$

This shows that the stress in the forming metal gets magnified to values considerably above the blast pressure in the water. The reflected wave in the water is shown as compression. Note that for a completely rigid boundary (instead of the aluminum) that the transmitted stress, σ_2', is twice the incident stress, σ_1. Steel is more rigid and nearly demonstrates this, see below.

Water to Steel

$$\sigma_1' = \frac{64,500 - 2060}{66,560} \quad \sigma_1 = .94\ \sigma_1$$

$$\sigma_2' = \frac{2\ (64,500)}{66,560} \quad \sigma_1 = 1.94\ \sigma_1$$

TABLE II

TRANSMISSIBILITY OF STRESS WAVES

MATERIALS	σ_1' (Reflected)	σ_2' Transmitted
Water to Die Steel	.94 σ_1	1.94 σ_1
Water to 2219 Aluminum	.85	1.85
2219 Aluminum to Die Steel	.43	1.43
2219 Aluminum to 2219 Aluminum	0	1.00
Die Steel to Die Steel	0	1.00
Die Steel to 2219 Aluminum	-.43	.57
Die Steel to Concrete	-.70	.30
Die Steel to Wood	-.92	.08
Die Steel to Water	-.94	.06
Die Steel to Air	-1.00	0

where σ_1 is the incident stress.

The peak impact stresses transmitted into the concrete under the tank are calculated to illustrate the procedure. An incident stress peak of 14,200 psi is assumed, as on Page 15 herein. Note that Ref. 1, Page 15, used 14,300 psi for the sample vibration analysis of the die.

Reflections, distortion or shear waves, and attenuations are all neglected in this analysis.

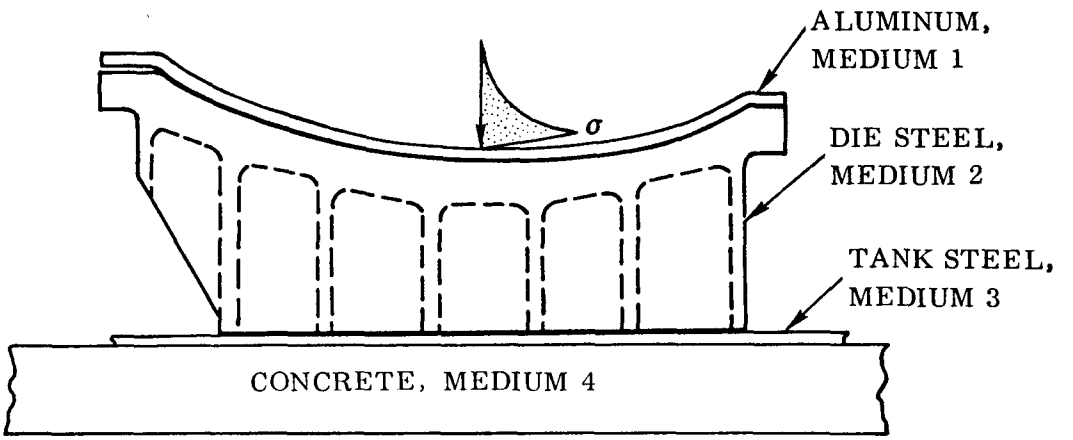

Figure 9 A Stress Wave Propagating Through the Blank, the Die, and the Explosive Forming Tank

σ_1, stress in aluminum, is 14,200 psi

σ_2', stress in die steel, is 1.43 (14,200) = 20,300 psi

σ_3', transmitted stress into the tank floor is assumed the same as the die steel, is 20,300 psi

σ_4', stress received is .30 σ_3' = .30 (20,300)
= 6100 psi

This stress is rather high for concrete on a static basis. It is not at all high compared with the critical-normal-fracture stress obtained from Equation 9 using v as the critical impact velocity (differential particle velocity).

Note that if the water pressure is 14,200 psi, the aluminum stress would be 14,200 x 1.85 = 26,300 psi. Hence, all the other stresses above would also be multiplied by 1.85.

6.0 EXPLOSIVE CHARGE LAYOUTS

The charge size and spacing is determined by methods of Ref. 1. A typical calculation of an over-all charge weight is made to illustrate the procedure. The data is from an actual jury-rigged shot on .63 thick 2219-T37 aluminum plate. A map of the charge is shown in Figure 11. The photo on Page 26 shows the actual charge loaded over the blank. Note the stretch press wedge clamp in lower right of the photo. The hoses in the photo are used to evacuate air from under the protective rubber blanket which covers the part.

The line numbers in Table III refer to Figure 11. The table gives the lengths of Primacord used in the charge. In this charge layout, four blasting caps are used, one in each corner. This aids in creating a symmetrical explosion. It is pointed out that with this pattern the water plume is very symmetrical and goes straight up about 150 feet with comparatively little water actually lost out of the tank. Also, the ground shake is very little when compared with unsymmetrical shots of much lower charge weights.

TABLE III

CHARGE WEIGHT CALCULATIONS

(1) LINE NO.	(2) LENGTH IN.	(3) CHARGE SIZE PER FOOT GR./FT.	(4) WEIGHT, LB. (2) x (3)/12 x 7000
1	60	1600	1.14
2	204	1600	3.88
3	355	800	3.48
4	80	200	.19
5	80	200	.19
6	74	200	.18
7	76	200	.18
8	10 x 4 = 40	400	.19
		Total	9.43 pounds

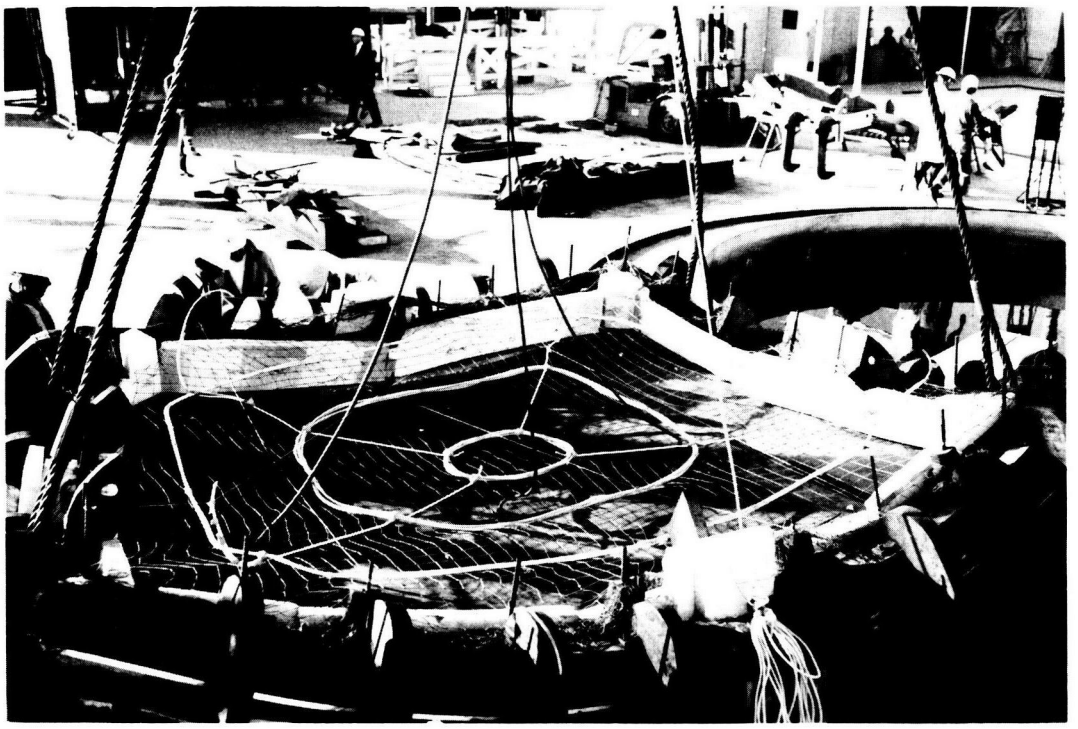

Figure 10 .63 Inch Thick 2219-T37 Aluminum Base Gore Jury-Rigged Shot - Note Fish Net Suspension

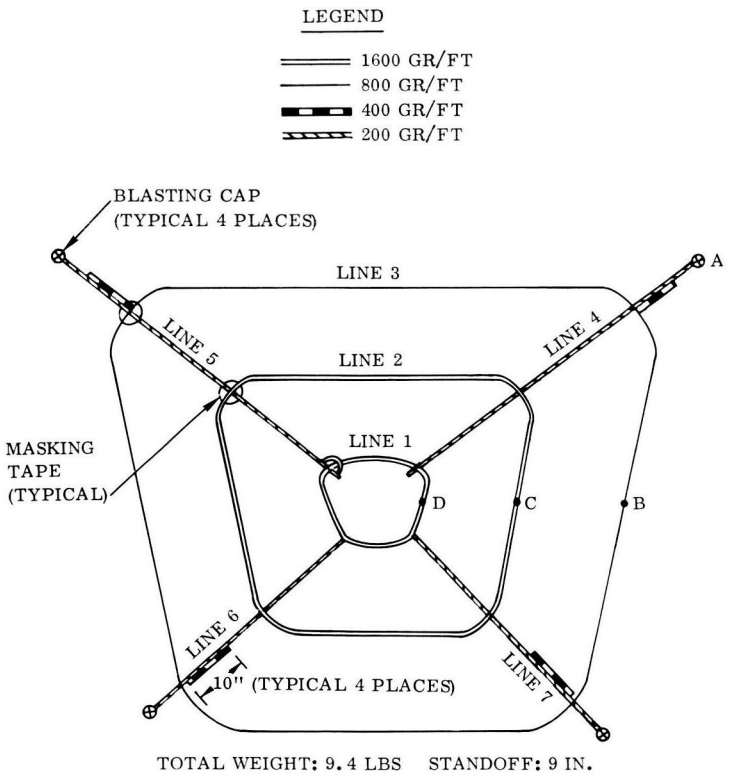

TOTAL WEIGHT: 9.4 LBS STANDOFF: 9 IN.

Figure 11 Shot No. 1 - .63 Inch Thick 2219-T37 Plate (12-17-63)

6.1 TIME FOR COMPLETING DETONATION

The time for detonation of points B, C, and D, (Figure 11) are arranged so they all fire at approximately the same time, since the distance from A to B is nearly the same as distance A-C and A-D as shown in Figure 12.

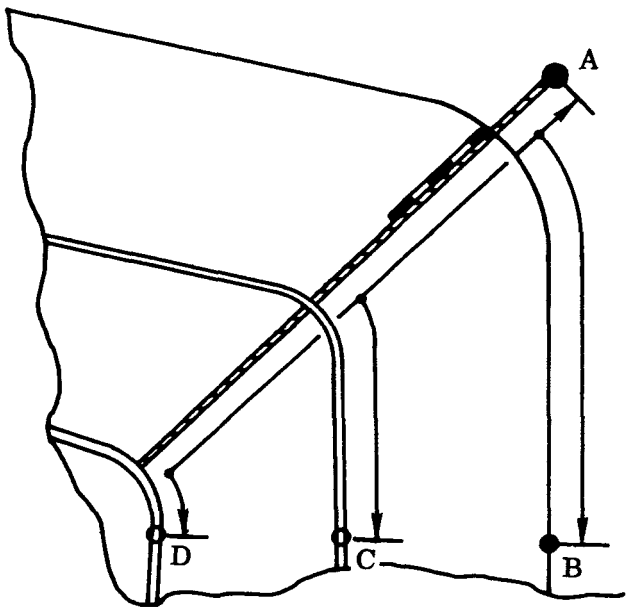

Figure 12 Primacord Lengths as Measured from One Blasting Cap

The Primacord always has the same rate of detonation which is highly reliable. Hence, when points B, C, and D fire simultaneously, the cancellations (Page 5), and multiplications (Page 39 of Ref. 1) will take place in the predicted manner. Table II of Ref. 1 lists the detonation speed of Primacord as well as the propagation speed of the fresh water shock wave. The total Primacord firing time is about 90 inches x 4 microseconds per inch = 360 microseconds.

The time for the water pressure wave to travel 9 inches through water is:

$$9/4750 \times 12 = .000158$$ which is 158 microseconds.

The squib (blasting cap) may take about 1000 microseconds to completely fire. This is quite long when compared to the Primacord detonation time of 360 microseconds.

The time it takes for the shock wave to travel through 7 feet of water to the tank wall is:

$$7/4750 = 1480$$ microseconds.

Speed of Sound in the Earth

The ground shake one feels in the vicinity of an explosive forming tank occurs after the metal forms. Hence, any instruments in the area will not be disturbed until after the metal is formed. The stress wave propagates through the earth at about 4000 feet per second. It will travel 100 feet in about .025 seconds.

6.2 SAMPLE CALCULATION

Figure 13 shows a sample view of some typical data recording instruments.

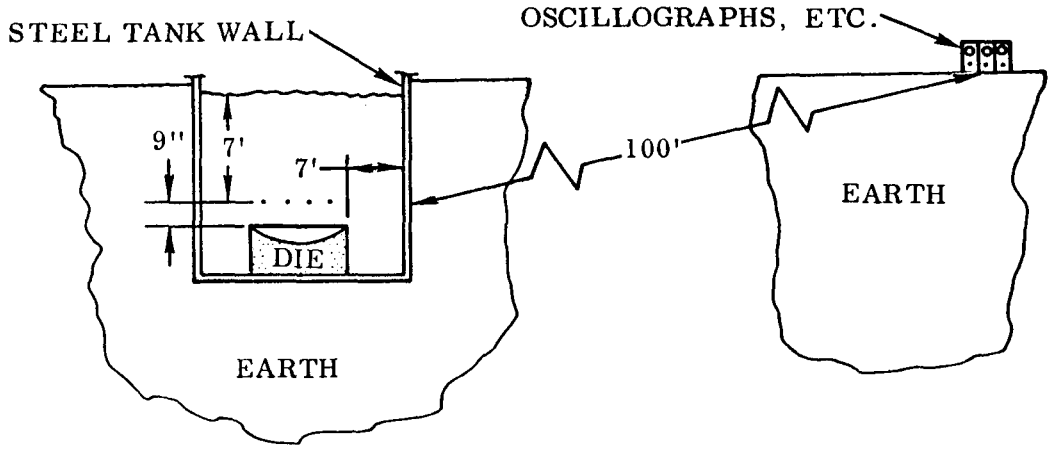

Figure 13 Relationship of Instrumentation to the Explosive Charge

The time from the initiation of Primacord detonation until the impulse hits the blank is 360 plus 158 = 518 microseconds.

The time from initiation of Primacord until ground stress wave disturbs the instruments is 360 + 1480 + 25, 000 = 26, 840 microseconds. The one-inch thick steel tank wall would add about 4 microseconds to this, which is negligible.

The forming time of the part (Page 14) is about .026 seconds. Add to this the 518 microseconds for detonation and shock wave travel. The time from initiation to completion of part forming then totals 26, 518 microseconds. Hence, it is advised that the instruments be located about 150 feet from the tank (instead of 100 feet as on Page 28) to insure that the ground stress wave will arrive after forming is complete. This

will minimize the disturbance of the data recorders during forming. The time from initiation then becomes:

$$360 + 1480 + 25,000 \times 1.5 = 39,340 \text{ microseconds.}$$

Rounded off, it is .0393 seconds for the earth wave to propagate to the instruments. The time for the part to be formed is .026 seconds.

Time to Travel Through the Air

The time for the sonic shock wave to travel 100 feet through the air is:

$$100/1100 = .091 \text{ seconds.}$$

Assuming 7 feet of water above the Primacord, the total time for the sound to be heard 100 feet away is $360 + 1480 + 91,000 = 92,840$ microseconds.

This is longer than it takes for the earth wave to travel, as would be expected because earth is much denser than air.

Electron Speed

The speed for the electrical signal to travel through wire from the tank to an oscillograph 150 feet away is calculated. The length of time for the pertinent forming events to take place may then be compared with this. Electrons travel 186,000 miles per second which is approximately 981×10^6 feet per second.

The time for a signal to travel 150 feet is:

$$150/981 \times 10^6 = .153 \text{ microseconds.}$$

Hence, the record will be completed long before any earth or air shock fronts reach the recording equipment.

7.0 CLAMPING

Static tests conducted during Phase I on various types of clamps, wedges, and frictional inserts, resulted in the selection of a type of self-energizing clamp as illustrated in Figure 14. Figure 14 shows the stretch press wedge clamp after static testing. The 2219-T37 sheet, .80 thick, is firmly wedged in place. This same general type of clamp was actually explosively tested (Figure 15) and found excellent during Phase II subscale die tests.

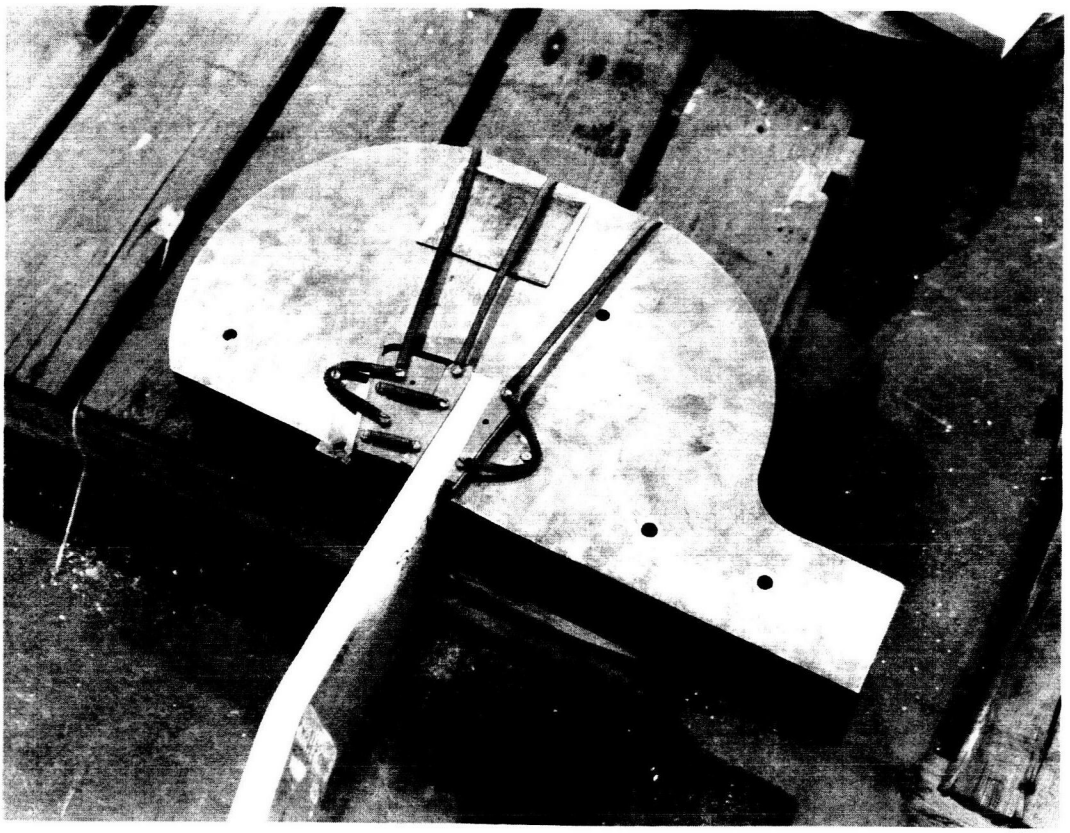

Figure 14 Stretch Press Wedge Clamp After Static Test

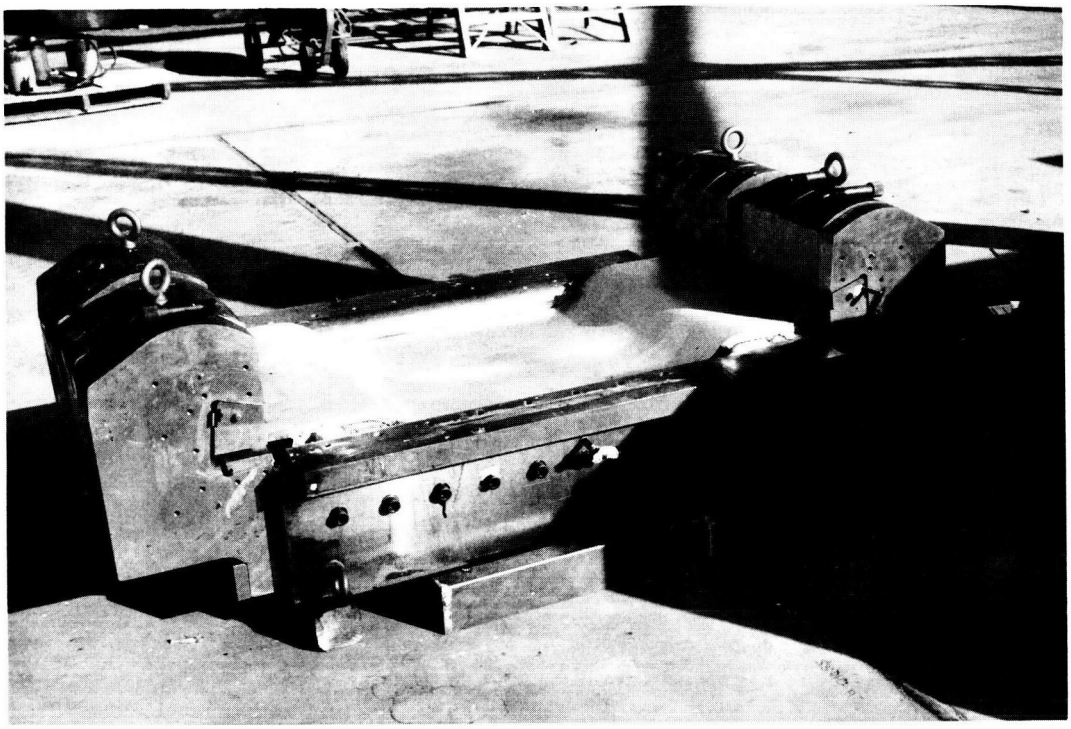

Figure 15 Sub-Scale Die Showing .89 Inch Thick 2219-T37 Plate After Explosive Forming

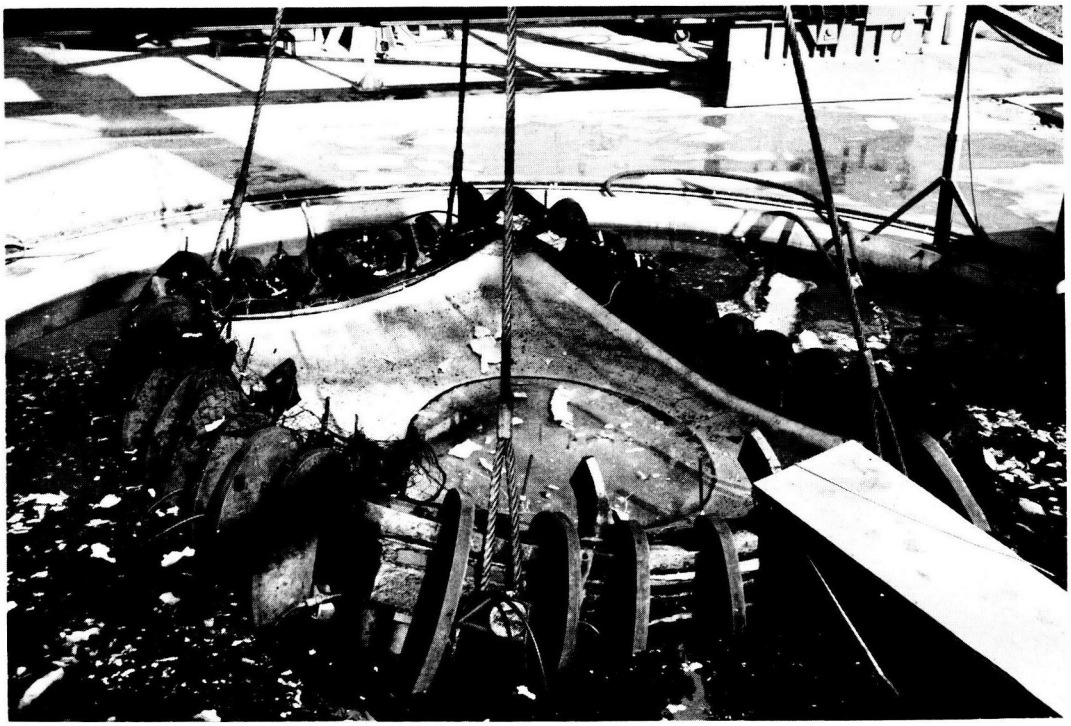

Figure 16 Base Gore After Forming - An Early Jury-Rigged Shot Using Only Hydraulic Jack Type Clamping.

8.0 CONCLUSIONS

Some techniques worked out in Phase II are:

- Foam blocks can be used to reduce pressures on objects that protrude 4 inches or more above the blank. In Phase III, the draw ring is intended to be only 2.5 inches thick. Hence, only a minimum amount of foam will be used, (Figure 10).

- Two types of clamps can be utilized to obtain varying clamping pressures around the blank periphery. Hydraulic jacks of 60 ton capacity are used for lighter clamps, (Figure 16). For larger loads, the stretch press wedge clamps may be used.

- Serrated steel wedges are the best for developing maximum friction in the clamps.

- The impulse method of analyzing an explosive-forming tank gives more reliable results than the pressure method of stress analysis.

- Symmetrical charges are recommended in the explosive forming tanks to promote even wear on the tank walls due to the blast pressures.

- The sub-scale die actually jumped laterally during an unsymmetrical explosive shot. The charge was not symmetrical with respect to the die. For this reason, caution should be used in the planning of unsymmetrically placed explosive charges.

9.0 REFERENCES

1. Johnson, R.W., "Report on Explosive Forming Technical Data", Ryan Aeronautical Co., Report No. 64B001, January, 1964.

2. Childers, G. and Wollner, G., "Structural Analysis of Explosion Forming Gore Die", Ryan Aeronautical Co., Report No. LD1-1, February, 1962.

3. Childers, G., "NASA 396 Inch Diameter Aluminum Bulkhead", Ryan Aeronautical Co., Progress Report No. 2, October, 1962.

4. Maleev, V.L., Machine Design, International Textbook Company, Scranton, Pa., 1939.

5a. Spangler, R.D., "Basic Design Features of A Nonimpacting, Pneumatically Drive, Hydraulically damped High Speed Tester", High Speed Testing - Vol. III, 3rd Annual Symposium, John Wiley and Sons, New York, October, 1961.

5b. Wolstenholme, W.E., "Characterizing Impact Behavior of Thermoplastics", see Ref. 5a, October, 1961

6. Cole, R., Underwater Explosions, Princeton University Press, 1948.

7. Wallen, H., "Proposal to Determine Optimum Forming, Tool Designs and Manufacturing Processes for 2219-T37 Gore Segments", Ryan Aeronautical Co., Report No. 63B093, September, 1963.

8. Rinehart, J. and Pearson, J., Explosive Working of Metals, MacMillan Company, New York, 1963.

9. Jacobsen, L. and Ayre, R., Engineering Vibrations, McGraw-Hill Book Company, New York, 1958.

10. Hawkins, K.D., "NASA 396 Inch Diameter Aluminum Bulkhead", Ryan Aeronautical Company, Progress Report No. 15, October, 1963.

11. Hawkins, K.D., Above, Progress Report No. 16, November, 1963.

12. Hawkins, K. D., Above, Progress Report No. 17, December, 1963.

13. Nadai, A., Theory of Flow and Fracture of Solids, V. I., McGraw-Hill Book Company, New York, 1950.

14. Rayleigh, Baron, The Theory of Sound, V. I. and II, Dover Publications, New York, 1945.

15. Ripperberger, E. A., and Abramson, H. N., "Reflection and Transmission of Elastic Pulses in a Bar at a Discontinuity", PROC. 3rd Midwestern Conference on Solid Mechanics, Univ. of Michigan Press, Ann Arbor, 1957.

16. Seely, P. B., and Smith, J. O., Advanced Mechanics of Materials, 2nd Edition, John Wiley and Sons, Inc., New York, 1952.

17. MIL-HDBK-5, Metallic Materials and Elements for Flight Vehicle Structures, August, 1962.

18. WADC-TR-53-7, June, 1953.

19. Timoshenko, S., Theory of Elasticity, McGraw-Hill Book Company, New York, 1934.

20. Oswatitsch, K., and Kuerti, G., Gas Dynamics, Academic Press, Inc., New York, 1956.

21. von Karman, Th., "On the Propagation of Plastic Deformation in Solids", NDRC-A-29, 1942.